Properties and thermal stability of chemically vapor deposited W-rich WSi x thin films

M. T. Wang, Y. C. Lin, M. S. Chuang, M. C. Chun, L. J. Chen, and M. C. Chen

Citation: Journal of Vacuum Science & Technology B **17**, 385 (1999); doi: 10.1116/1.590567
View online: http://dx.doi.org/10.1116/1.590567
View Table of Contents: http://scitation.aip.org/content/avs/journal/jvstb/17/2?ver=pdfcov
Published by the AVS: Science & Technology of Materials, Interfaces, and Processing

---

Properties and thermal stability of chemically vapor deposited W-rich WSi$_x$ thin films*

M. T. Wang, Y. C. Lin, and M. S. Chuang
Department of Electronics Engineering, National Chiao-Tung University, Hsinchu, Taiwan

M. C. Chun
National Nano Device Laboratory, 1001 Ta Hsueh Rd., Hsinchu, Taiwan

L. J. Chen
Department of Submicron Technology Development, ERSO/ITRI, Hsinchu, Taiwan

M. C. Chen[a)]
Department of Electronics Engineering, National Chiao-Tung University, Hsinchu, Taiwan

(Received 27 February 1998; accepted 18 December 1998)

The tungsten-rich (Si/W atomic ratio less than 2.0) chemical vapor deposition (CVD)-WSi$_x$ layer was found to be an efficient diffusion barrier against Cu diffusion. In this study, the properties and thermal stability of the W-rich WSi$_x$ films chemically vapor deposited at various deposition temperatures, pressures, and SiH$_4$/WF$_6$ reactant gas flow ratios were investigated. With SiH$_4$/WF$_6$ flow rates of 6/2 sccm and a total gas pressure of 12 mTorr, the activation energy of the CVD process was determined to be 3.0 kcal/mole, and the film deposited at 250 °C has a Si/W atomic ratio of unity. The WSi$_x$ films have a low residual stress, low electrical resistivity, and excellent step coverage. For the WSi$_x$ layers deposited on Si substrates, the residual stress varies from 7 to 9 $\times 10^8$ dynes/cm^2 depending on the deposition temperature. The resistivity of the WSi$_x$ films varies from 200 to 340 $\mu\Omega$ cm; higher deposition temperatures and SiH$_4$/WF$_6$ flow ratios resulted in higher film resistivities. The as-deposited amorphous WSi$_x$ layer is thermally stable up to 600 °C; however, crystallization of the deposited film takes place at 650 °C and WSi$_x$ was transformed into WSi$_2$ phase when the WSi$_x$/Si structure was thermally annealed at temperatures above 650 °C. © *1999 American Vacuum Society.* [S0734-211X(99)03602-1]

I. INTRODUCTION

It was found recently that a tungsten-rich (Si/W atomic ratio less than 2.0) chemical vapor deposition (CVD)-WSi$_x$ layer served efficiently as diffusion barrier against Cu diffusion.[1,2] The thermal stability of Cu/WSi$_x$(50 nm)/p^+-n junction diodes was found to reach 500 °C; with an *in situ* N$_2$ plasma treatment on the surface of WSi$_x$ layers, the resultant Cu/WSiN/WSi$_x$(50 nm)/p^+-n junction diodes were able to retain integrity of their electrical characteristics up to at least 600 °C.[2] Moreover, the tungsten-rich CVD-WSi$_x$ films were found to have a low residual stress, low electrical resistivity, and excellent step coverage. This indicates that the tungsten-rich CVD-WSi$_x$ films possess great potential in application to Cu metallization system. Thus, a systemic study of tungsten-rich CVD-WSi$_x$ films is vital to their applications in ultralarge scale integration (ULSI) circuits.

Refractory metal silicides have been intensively studied for potential use as interconnection in ULSI circuits.[3,4] These materials offer good thermal stability and good electrical conductivity. Among them, tungsten silicide (WSi$_x$) is one of the most promising materials because of its good compatibility with conventional ULSI fabrication processes.[5–21] Sputter deposited WSi$_x$ films have been widely used in integrated circuits (ICs) manufacture.[4,6] In general, the sputter deposited WSi$_x$ used in ICs manufacture has a Si/W atomic ratio larger than 2.0, and is often referred to as ''silicon-rich WSi$_x$.'' The as-sputtered WSi$_x$ films have a resistivity of 600–900 $\mu\Omega$ cm, which decreases to about 50 $\mu\Omega$ cm after annealing at 1000 °C.[6] However, it is difficult to deposit WSi$_x$ films, with acceptable step coverage, into contact holes of deep subhalf micron dimensions using physical vapor deposition (PVD) method. In contrast, CVD method generally offers superior step coverage of conformal deposition; thus chemically vapor deposited WSi$_x$ (CVD-WSi$_x$) layer is becoming very attractive in ULSI application.[5]

The first systemic study of CVD-WSi$_x$, to our knowledge, was done by Brors *et al.*,[7] they proposed to deposit WSi$_x$ films in a cold wall reactor using SiH$_4$/WF$_6$ as reactive gas mixtures and obtained a good quality silicide films with a resistivity as low as 30 $\mu\Omega$ cm after a postdeposition annealing treatment. It was reported that the residual stress in CVD-WSi$_x$ films decreased linearly with increasing silicon content in the WSi$_x$ film.[2,22] In addition, it was found that the resistivity of as-deposited CVD-WSi$_x$ film increased with increasing deposition temperature.[7,13,22] Although many studies have been dedicated to the properties and thermal stability of silicon-rich (Si/W atomic ratio larger than 2.0) nonstoichiometric CVD-WSi$_x$ films, little work has been done on the tungsten-rich CVD-WSi$_x$ layers.

In this study, the properties and thermal stability of tungsten-rich nonstoichiometric CVD-WSi$_x$ thin films were systemically investigated. The WSi$_x$ thin layers were depos-

---

*No proof corrections received from author prior to publication.

[a)] Electronic mail: mcchen@cc.nctu.edu.tw

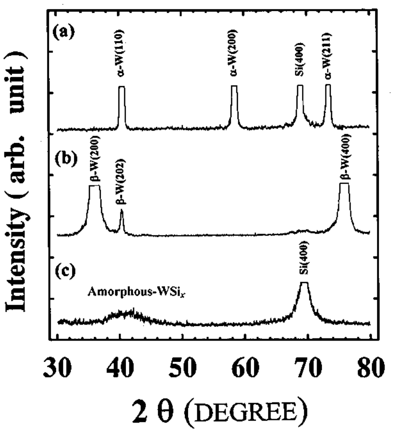

FIG. 1. XRD spectra of WSi$_x$ films deposited on bare Si substrate with SiH$_4$/WF$_6$ flow ratio of (a) 0.25, (b) 1.5, and (c) 3.0. The films were deposited at 300 °C with a total gas pressure of 20 mTorr.

ited by low pressure chemical vapor deposition (LPCVD) method using the SiH$_4$ reduction of WF$_6$. The properties of CVD-WSi$_x$ layers including crystalline phase, deposition rate, electrical resistivity, residual stress, surface roughness, and step coverage were investigated. The thermal stability of CVD-WSi$_x$ layers was also investigated using various techniques [scanning electron microscopy (SEM), x-ray diffraction (XRD) analyses, Rutherford backscattering spectroscopy (RBS), and sheet resistance measurements]. The results of this study might be useful in multilevel metallization for ULSI circuits.

II. EXPERIMENT

The test samples were fabricated on *n* type, (100)-oriented, 4-in.-diam silicon wafers with 4–7 Ω cm nominal resistivity. After RCA standard cleaning, one group of wafers was thermally oxidized to grow a 500-nm-thick SiO$_2$ layer. Unpatterned samples of WSi$_x$/Si and WSi$_x$/SiO$_2$/Si structures were then prepared for material analysis. For step coverage study, patterned samples with trenches having aspect ratios ranging from 1 to 4 were also prepared.

The WSi$_x$ layers were deposited by CVD method using SiH$_4$ reduction of WF$_6$. Prior to the WSi$_x$ deposition, both the bare Si and SiO$_2$/Si wafers were dipped in dilute HF (50:1) for 30 s, followed by a rinse in DI water for 3 min and spin dry. The wafers were then loaded into a load-locked cold wall CVD system within 5 min and transferred by a robot arm to the deposition chamber without exposure to the atmosphere. The base pressure of the CVD chamber was 10^{-6} Torr. In this study, WSi$_x$ films were chemically vapor deposited from SiH$_4$/WF$_6$ gas mixtures with the conditions illustrated as follows: substrate temperature 150–450 °C, total gas pressure 12–20 mTorr, WF$_6$ flow rate 2 sccm, and SiH$_4$ flow rate 4–100 sccm.

The properties of the CVD-WSi$_x$ layers including crystalline phase, deposition rate, electrical resistivity, residual stress, surface roughness, and step coverage were investigated. The samples of the WSi$_x$/Si and WSi$_x$/SiO$_2$/Si structures were thermally annealed in N$_2$ flowing furnace for 30 min at a temperature ranging from 400 to 800 °C. The variation of sheet resistance with respect to the annealing temperature was used to monitor the thermal stability. Atomic force microscopy (AFM) was employed to characterize the surface roughness. XRD analysis was used for phase identification. RBS was used to determine the Si/W atomic ratio of WSi$_x$ films and to examine the interdiffusion between W and Si substrate at the WSi$_x$/Si interface. Moreover, SEM was employed to measure the film thickness and observe the surface morphology as well as the change of microstructure.

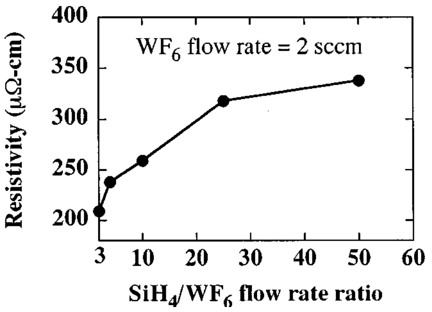

FIG. 2. Resistivity of WSi$_x$ films vs SiH$_4$/WF$_6$ flow ratio. The WSi$_x$ films were deposited at 250 °C with a total gas pressure of 12 mTorr and WF$_6$ flow rate of 2 sccm.

III. RESULTS AND DISCUSSION

A. Properties of CVD-WSi$_x$ thin films

1. Effects of SiH$_4$/WF$_6$ flow rate

Three different types of film microstructure, α-W phase, β-W phase, and amorphous WSi$_x$ phase, were obtained by the SiH$_4$ reduction of WF$_6$ with different SiH$_4$/WF$_6$ flow ratio, as revealed by XRD analysis (Fig. 1). At a substrate temperature of 300 °C and with a total gas pressure of 20 mTorr, α-W diffraction peaks were detected for films deposited with SiH$_4$/WF$_6$ flow ratio lower than 1.0 [Fig. 1(a)], while β-W peaks were detected for films deposited with SiH$_4$/WF$_6$ flow ratio ranging from 1.0 to 1.5 [Fig. 1(b)]. With the SiH$_4$/WF$_6$ flow ratio higher than 2, the structure of WSi$_x$ films was eventually amorphous [Fig. 1(c)].

To investigate the effects of SiH$_4$/WF$_6$ flow ratio on the resistivity and Si/W atomic ratio of WSi$_x$ films, the CVD

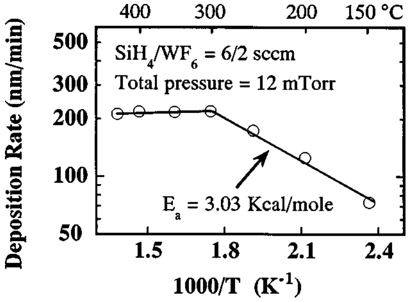

FIG. 3. Deposition rate of WSi$_x$ films vs deposition temperature. The WSi$_x$ films were deposited with a total gas pressure of 12 mTorr and SiH$_4$/WF$_6$ flow rates of 6/2 sccm.

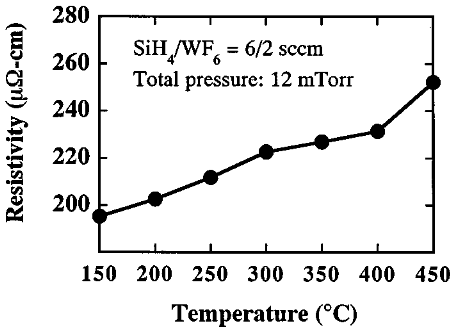

FIG. 4. Resistivity of WSi$_x$ films vs deposition temperature. The WSi$_x$ films were deposited at a total gas pressure of 12 mTorr and SiH$_4$/WF$_6$ flow rates of 6/2 sccm.

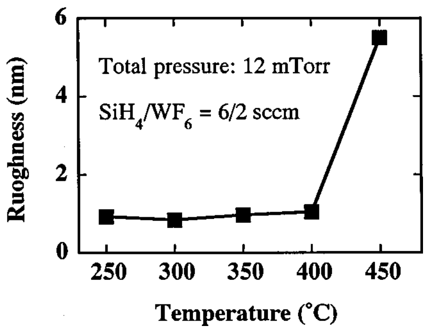

FIG. 6. Surface roughness of as-deposited CVD-WSi$_x$ films vs deposition temperature. The WSi$_x$ films were deposited at a total gas pressure of 12 mTorr and SiH$_4$/WF$_6$ flow rates of 6/2 sccm.

process was conducted at a substrate temperature of 250 °C and with a SiH$_4$ flow rate ranging from 4 to 100 sccm, while keeping the WF$_6$ flow rate at 2 sccm and the total gas pressure at 12 mTorr. Figure 2 shows the resistivity of CVD-WSi$_x$ films versus SiH$_4$/WF$_6$ flow ratio. The resistivity of WSi$_x$ layers increases with increasing flow ratio of SiH$_4$/WF$_6$; this increase in resistivity is presumably related to an increased amount of Si incorporated in the WSi$_x$ layer. We found that the Si/W atomic ratio in the WSi$_x$ layer increased from 1.0 to 1.3 as the SiH$_4$/WF$_6$ flow ratio was increased from 3 to 50, as determined by RBS measurements. Similar results were reported by Clark, although the SiH$_4$/WF$_6$ flow ratio ranged from 85 to 315, deposition temperature ranged from 330 to 360 °C and the resultant WSi$_x$ layer was nonstoichiometric silicon-rich ($x>2$) in his study.[22]

2. Deposition temperature effect

The CVD of WSi$_x$ films was conducted at temperatures ranging from 150 to 450 °C with a total gas pressure of 12 mTorr, WF$_6$ flow rate of 2 sccm, and SiH$_4$ flow rate of 6 sccm. Figures 3 and 4 show the deposition rate and resistivity of WSi$_x$ films versus deposition temperature. Below 300 °C, the surface reaction might be the rate limiting process, and the activation energy of the CVD process was determined to be 3.0 kcal/mole. At temperatures above 300 °C, the deposition rate was independent of the substrate temperature; as a result, the process was possibly controlled by mass transfer mechanism. Thermodynamically, silane is an unstable compound and will decompose into silicon and hydrogen. Since the decomposition of SiH$_4$ is a thermally activated process, the amount of Si incorporated into WSi$_x$ films will increase with increasing deposition temperature. It was reported that the resistivity of chemically vapor deposited amorphous WSi$_x$ films increased with increasing Si content in the as-deposited films.[20,22] The reported observation is thus consistent with the results of this work that the increase in deposition temperature resulted in an increase in resistivity for the as-deposited WSi$_x$ films.

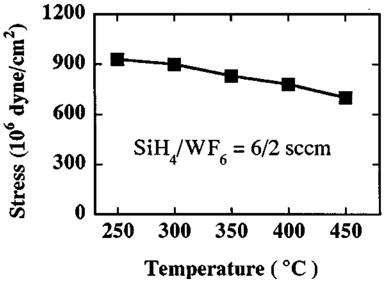

FIG. 5. Residual stress in as-deposited WSi$_x$ films as a function of deposition temperature. The WSi$_x$ films were deposited at a total gas pressure of 12 mTorr and SiH$_4$/WF$_6$ flow rates of 6/2 sccm.

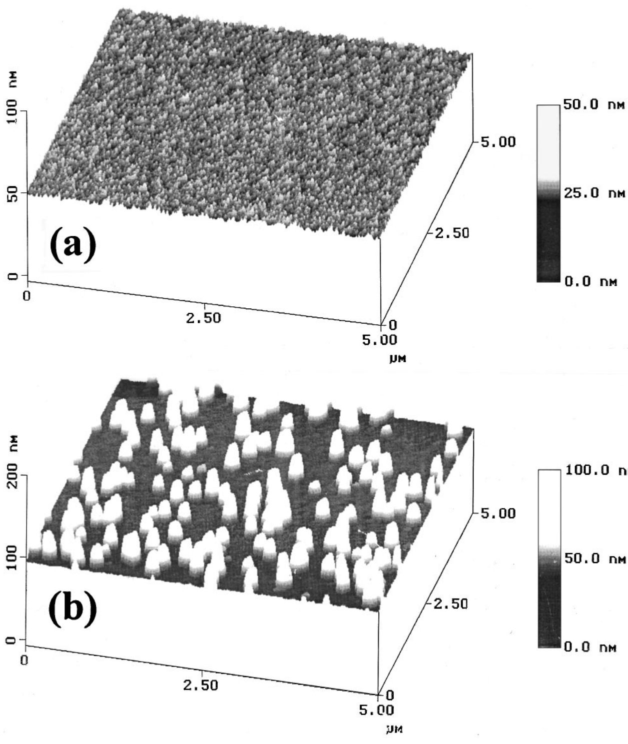

FIG. 7. AFM micrographs for WSi$_x$ films deposited at substrate temperature of (a) 250 and (b) 450 °C.

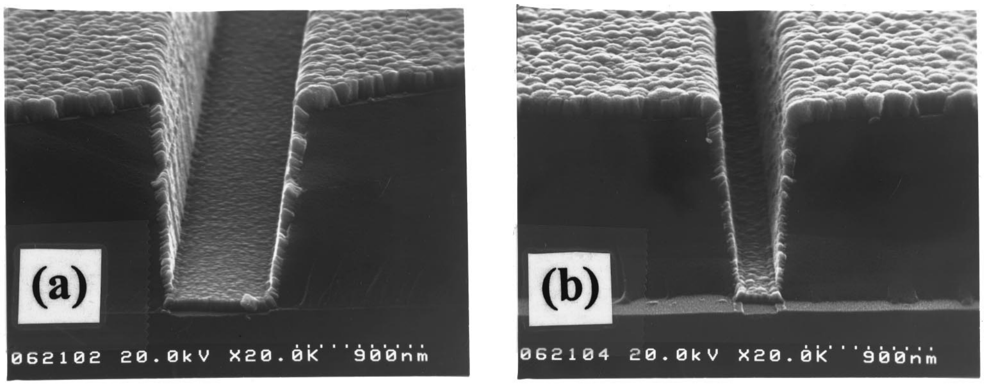

FIG. 8. Step coverage of WSi_x films deposited on submicron trenches with aspect ratio of (a) 2.0 and (b) 4.0.

3. Residual stress

The residual stress was measured using a Tencor's FLX-2320 system. The value of stress was determined according to Eq. (1),

$$\sigma = \frac{E}{6(1-\nu)} \frac{t^2}{d} \left[\frac{1}{R} - \frac{1}{R_0} \right], \tag{1}$$

where σ is the stress, E is the Young's modulus of Si substrate, ν is the Poisson ratio of Si substrate, t is the thickness of WSi_x film, d is the thickness of Si substrate, while R_0 and R are the radii of curvature of the substrate before and after the film deposition, respectively.

Figure 5 shows the residual stress in as-deposited WSi_x films versus deposition temperature. The stress decreases slightly with increasing deposition temperature. This is presumably due to larger amount of Si incorporated in the WSi_x layer at higher deposition temperatures. This result agrees with the reported work in literature that the stress of WSi_x is influenced by the Si/W atomic ratio in the WSi_x film.[22,23]

It should be noted that a good adherence can be obtained for the CVD-WSi_x layer deposited on Si substrate at temperatures higher than 200 °C. Peeling of WSi_x layer on Si substrate was found for the WSi_x layer deposited at 150 °C to a thickness of 220 nm. Moreover, peeling of WSi_x layer on SiO_2 was found for the WSi_x layer deposited at 200 °C.

4. Surface roughness

The surface roughness of CVD-WSi_x films was measured using AFM on unpatterned WSi_x/Si samples. Figure 6 shows the surface roughness versus deposition temperature for as-deposited CVD-WSi_x layers. A fairly smooth surface was obtained for the WSi_x films deposited at temperatures between 250 and 400 °C, as analyzed using AFM [Fig. 7(a)]. However, the surface roughness increased drastically for the films deposited at temperatures above 450 °C [Fig. 7(b)]. Particles generated by gas phase nucleation might lead to the surface roughness. It has been reported that the gas phase nucleation occurred at temperatures above 400 °C and with SiH_4/WF_6 flow ratio higher than unity. Moreover, it was found that the particle generation rate increased with increasing deposition pressure.[24]

5. Step coverage

A highly conformal deposition of CVD-WSi_x films was obtained. Figure 8 shows the WSi_x films deposited on submicron trenches with aspect ratios of 2 and 4 using the deposition condition illustrated as follows: substrate temperature 250 °C, total gas pressure 12 mTorr, WF_6 flow rate 2 sccm, and SiH_4 flow rate 6 sccm. We referred to this condition as ''standard deposition condition'' hereafter.

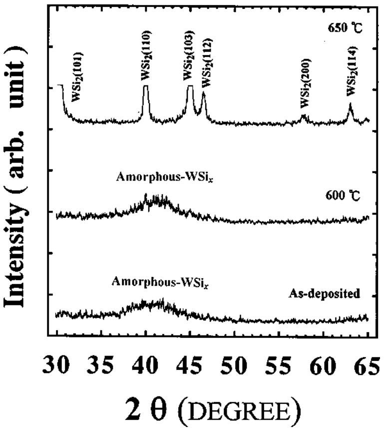

FIG. 9. XRD spectra for as-deposited and thermally annealed WSi_x(220 nm)/Si samples.

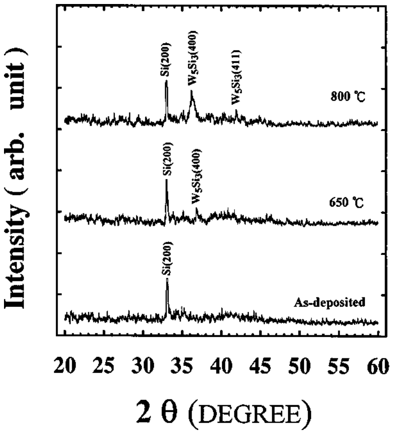

FIG. 10. XRD spectra for as-deposited and thermally annealed WSi_x(50 nm)/SiO_2/Si samples.

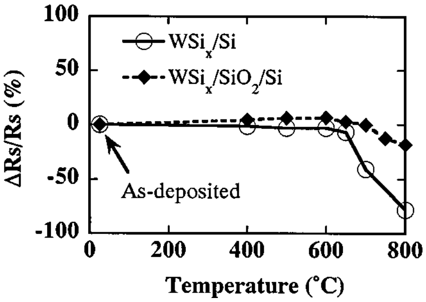

FIG. 11. Sheet resistance change vs annealing temperature for WSi$_x$/Si and WSi$_x$/SiO$_2$/Si samples.

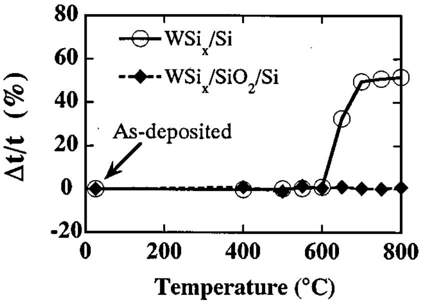

FIG. 12. Thickness change of WSi$_x$ layer vs annealing temperature for WSi$_x$/Si and WSi$_x$/SiO$_2$/Si samples.

B. Thermal stability of CVD-WSi$_x$ films

The thermal stability of the WSi$_x$ layers, deposited using the standard deposition condition on bare Si and SiO$_2$/Si substrates to produce WSi$_x$(220 nm)/Si and WSi$_x$(50 nm)/SiO$_2$/Si structures, respectively, was investigated using the techniques of XRD, RBS, SEM, and the sheet resistance measurement.

1. XRD analyses

For WSi$_x$(220 nm)/Si samples, the as-deposited WSi$_x$ films are amorphous, as indicated by XRD analysis shown in Fig. 9. A broad peak was present clearly at 2θ angle of 39°–43°. Since at least six diffraction peaks available to various phases (110-α-W, 330-W$_5$Si$_3$, 202-W$_5$Si$_3$, 420-W$_5$Si$_3$, 411-W$_5$Si$_3$, and 110-WSi$_2$) are located within this 2θ range, it is not possible to draw any conclusion from the position of this broad peak. After annealing at 600 °C, the WSi$_x$ layer retained its original amorphous phase. However, a number of diffraction peaks belonging to WSi$_2$ phase appeared after the sample was annealed at 650 °C. The presence of WSi$_2$ phase indicates that reaction occurred at the WSi$_x$/Si interface.

XRD spectra for as-deposited and thermally annealed WSi$_x$(50 nm)/SiO$_2$/Si samples are illustrated in Fig. 10. After annealing at 650 °C, a very weak peak of W$_5$Si$_3$ phase appeared at 2θ angle of about 37°, and the intensity of the W$_5$Si$_3$ peaks increased with increasing annealing temperature. However, no peak of WSi$_2$ phase was observed even after annealing at 800 °C. This different behavior between the WSi$_x$/Si and WSi$_x$/SiO$_2$/Si structures is apparently related to the presence of SiO$_2$ layer in the latter structure. The SiO$_2$ layer prevented out diffusion of Si atoms from the sub-

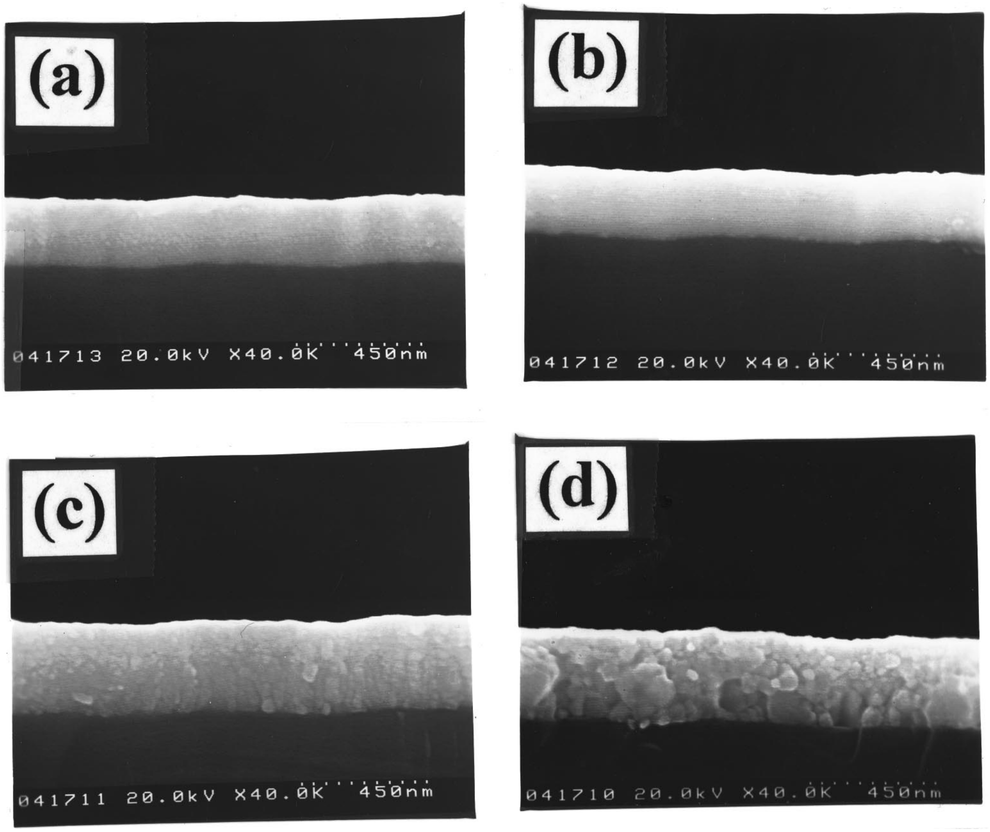

FIG. 13. Cross-sectional SEM micrographs for WSi$_x$/Si samples (a) as-deposited, and thermally annealed at (b) 600, (c) 650, and (d) 800 °C.

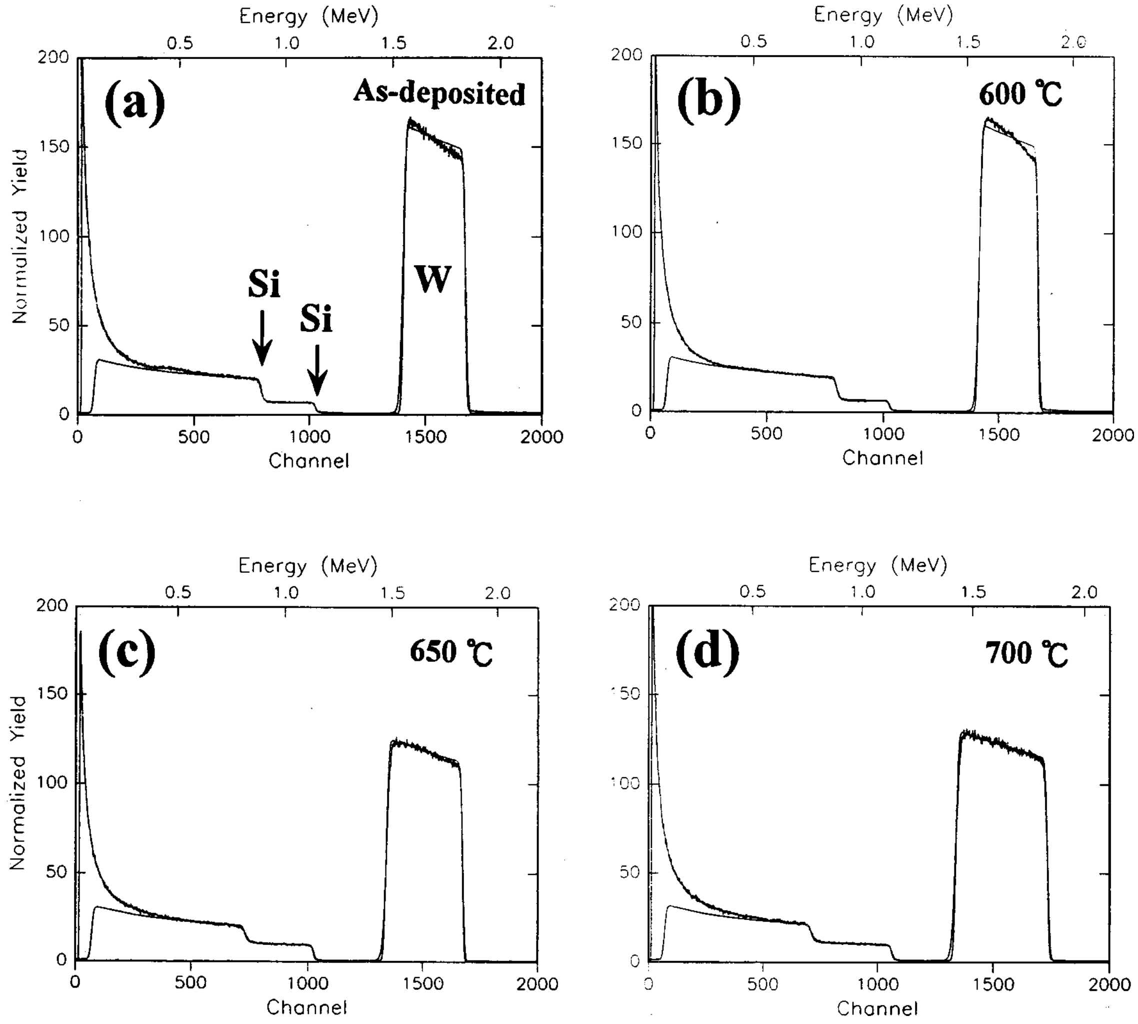

FIG. 14. Rutherford backscattering spectra for WSi$_x$/Si samples (a) as-deposited, and thermally annealed at (b) 600, (c) 650, and (d) 700 °C.

strate to the WSi$_x$ layer; thus, the Si deficient WSi$_x$ layer was not able to form stable WSi$_2$ phase during thermal annealing. Moreover, since no signal of WSi$_2$ phase was observed for the thermally annealed WSi$_x$/SiO$_2$/Si sample, we excluded the possibility that the as-deposited WSi$_x$ film contained amorphous WSi$_2$. Therefore, we conclude that the as-deposited WSi$_x$ is a mixture of amorphous phase of W and Si, together with possible existence of amorphous phase of W$_5$Si$_3$.[6]

2. Sheet resistance measurements

The sheet resistance change of annealed samples, normalized to the as-deposited sheet resistance value, is denoted as $\Delta Rs/Rs$ (%) and defined as follows:

$$\frac{\Delta Rs}{Rs}(\%)=\left[\frac{Rs_{\text{after anneal}}-Rs_{\text{as-deposited}}}{Rs_{\text{as-deposited}}}\right]\times 100\%. \tag{2}$$

Figure 11 shows the sheet resistance change versus annealing temperature for the WSi$_x$/Si and WSi$_x$/SiO$_2$/Si samples, in which the WSi$_x$ layers were deposited using the standard deposition condition. The sheet resistance of WSi$_x$/Si remained constant up to 600 °C, implying that the amorphous structure of WSi$_x$ film remained unchanged, as confirmed by XRD patterns shown in Fig. 9. With the samples annealed at temperatures above 650 °C, the sheet resistance decreased rapidly with increasing annealing temperature. This is attributed to the formation of the low resistivity WSi$_2$ phase at temperatures above 650 °C (Fig. 9). For WSi$_x$(50 nm)/SiO$_2$/Si samples, the sheet resistance also showed decreasing trend after annealing at temperatures above 650 °C; however, the extent of decrease is much smaller than the WSi$_x$/Si samples. The decrease in sheet resistance was presumably due to crystallization and grain growth of W$_5$Si$_3$ phase (Fig. 10).

3. Thickness change of WSi$_x$ layers

The thermal annealing was found to result in the thickness change of WSi$_x$ layers for WSi$_x$/Si samples. The thickness change normalized to the as-deposited thickness is denoted as $\Delta t/t$ (%) and defined as follows:

$$\frac{\Delta t}{t}(\%)=\left[\frac{t_{\text{after anneal}}-t_{\text{as-deposited}}}{t_{\text{as-deposited}}}\right]\times 100\%, \tag{3}$$

where t is the thickness of WSi$_x$ layers.

Figure 12 shows the thickness change of WSi$_x$ layers for the WSi$_x$/Si and WSi$_x$/SiO$_2$/Si samples after annealing at various temperatures. The thickness of WSi$_x$ layers for WSi$_x$/Si samples remained constant after annealing at temperatures up to 600 °C; however, the thickness made a significant increase at temperatures above 600 °C and the normalized increase finally reached a saturated value of about 50% when the sample was annealed at temperatures above 700 °C. This is consistent with the results of XRD analysis (Fig. 9) and sheet resistance measurements (Fig. 11) that WSi$_2$ phase was formed at temperatures above 600 °C. For WSi$_x$/SiO$_2$/Si samples, the thickness of WSi$_x$ layers showed no obvious change after thermal annealing at temperatures up to 800 °C. Figure 13 shows the cross sectional SEM micrographs for WSi$_x$/Si samples before and after thermal annealing. The increase in thickness of WSi$_x$ layers was clearly observed for WSi$_x$/Si samples annealed at temperatures above 650 °C. Moreover, the amorphous phase of the as-deposited WSi$_x$ layer became a grain-like structure, presumably related to the WSi$_2$ grains.

4. RBS analyses

The observed spectra from 2.0 MeV He$^+$ RBS measurements for the as-deposited and thermally annealed WSi$_x$/Si samples are illustrated in Fig. 14. The as-deposited sample exhibits one RBS peak of channeling energies relating to W in the WSi$_x$ layer, and two edges which relate to, respectively, the Si in the WSi$_x$ layer (at about 1.12 MeV) and the Si substrate (at about 0.88 MeV) [Fig. 14(a)]. After annealing at 600 °C, no obvious change in the RBS spectrum was observed [Fig. 14(b)]. The Si/W atomic ratio of as-deposited WSi$_x$ layers was determined to be 1.0 and remained unchanged after annealing at 600 °C. This suggests that the WSi$_x$/Si structure remained stable up to at least 600 °C. After annealing at 650 °C, the width of the W peak increased, indicating an increase in thickness of the W containing layer [Fig. 14(c)]. Upon annealing at 700 °C, the width of the W peak increased to about 1.5 times the original width [Fig. 14(d)]. This is consistent with our previous results of the increase in the WSi$_x$ thickness shown in Fig. 12. The Si/W atomic ratio was determined to be 66/34 and a small increase in Si peak intensity at backing energy of 1.12 MeV was also observed, indicating the increase of Si/W atomic ratio for the WSi$_x$ layer. This clearly indicates the transformation of WSi$_x$ into WSi$_2$ phase.

IV. SUMMARY

The properties and thermal stability of W-rich CVD-WSi$_x$ thin films were investigated. We found that the WSi$_x$ layers have a low stress, low electrical resistivity, and excellent step coverage. For WSi$_x$ layers deposited on Si substrates, the stress varies from 7 to 9×10^8 dynes/cm^2 depending on the deposition temperature. The resistivity of the WSi$_x$ films varies from 200 to 340 $\mu\Omega$ cm; higher deposition temperatures and SiH$_4$/WF$_6$ flow ratios resulted in higher film resistivities. With SiH$_4$/WF$_6$ flow rates of 6/2 sccm and a total gas pressure of 12 mTorr, the activation energy of the CVD process was determined to be 3.0 kcal/mole, and the WSi$_x$ film deposited at a temperature of 250 °C has a Si/W atomic ratio of unity. As for the thermal stability of CVD-WSi$_x$ films, we found that the WSi$_x$/Si contact system is thermally stable up to at least 600 °C. However, WSi$_x$ was transformed into WSi$_2$ phase when the WSi$_x$/Si structure was thermally annealed at temperatures above 650 °C.

ACKNOWLEDGMENT

This work was supported by the National Science Council (ROC) under Contract No. NSC86-2215-E-009-040.

[1] M. T. Wang, Y. C. Lin, J. Y. Lee, C. C. Wang, and M. C. Chen, J. Electrochem. Soc. (to be published).

[2] M. T. Wang, Y. C. Lin, J. Y. Lee, C. C. Wang, and M. C. Chen (unpublished).

[3] T. P. Chow and A. J. Steckl, IEEE Trans. Electron Devices **ED-30**, 1480 (1983).

[4] S. P. Murarka, J. Vac. Sci. Technol. **17**, 775 (1980).

[5] J. E. J. Schmitz, *Chemical Vapor Deposition of Tungsten and Tungsten Silicides for VLSI/ULSI Applications* (Noyes, Park Ridge, NJ, 1992), pp. 171–208.

[6] S. R. Wilson, C. J. Tracy, and J. L. Freeman, Jr., *Handbook of Multilevel Metallization for Integrated Circuits: Materials, Technology, and Applications* (Noyes, Park Ridge, NJ, 1993), pp. 53–55.

[7] D. L. Brors, J. A. Fair, K. A. Monnig, and K. C. Saraswat, Solid State Technol. **26**, 183 (1983).

[8] M. Suzuki, N. Kobayashi, and K. Mukai, *Tungsten and Other Advanced Metals for VLSI/ULSI Applications V*, edited by S. S. Wang and S. Furukawa (Materials Research Society, Pittsburgh, PA, 1990), pp. 259–265.

[9] D. L. Brors, J. A. Fair, and K. Monnig, Semiconductor International, May 1984 (unpublished), p. 82.

[10] S. Sachdev and R. Castellano, Semiconductor International, May 1985 (unpublished), p. 306.

[11] R. Togei, J. Appl. Phys. **59**, 3582 (1986).

[12] M. Kottke, F. Pintchovski, T. R. White, and P. J. Tobin, J. Appl. Phys. **60**, 2835 (1986).

[13] Y. Shioya, T. Itoh, I. Kobayashi, and M. Maeda, J. Electrochem. Soc. **133**, 1475 (1986).

[14] Y. Shioya and M. Maeda, J. Appl. Phys. **60**, 327 (1986).

[15] C. Bernard, R. Madar, and Y. Pauleau, Semicond. Sci. Technol. **32**, 79 (1989).

[16] K. C. Saraswat, D. L. Brors, J. A. Fair, K. A. Monnig, and R. Beyers, IEEE Trans. Electron Devices **ED-30**, 1497 (1983).

[17] D. K. Sadana, A. E. Morgan, M. H. Norcott, and S. Naik, J. Appl. Phys. **62**, 2830 (1987).

[18] D. Dobkin, L. Bartholomew, G. McDaniel, and J. DeDontney, J. Electrochem. Soc. **137**, 1623 (1990).

[19] M. Suzuki, N. Kobayashi, K. Mukai, and S. Kondo, J. Electrochem. Soc. **137**, 3213 (1990).

[20] J. H. Sone and H. J. Kim, in *Advanced Metallization and Processing for Semiconductor Devices and Circuits*, edited by A. Katz, S. P. Murarka, Y. I. Nissim, and James M. E. Harper (Materials Research Society, Pittsburgh, PA, 1990), Vol. 260, pp. 621–626.

[21] N. Thomas, A. M. Dutron, C. Vahlas, C. Bernard, and R. Madar, J. Electrochem. Soc. **142**, 1608 (1995).

[22] T. E. Clark, J. Vac. Sci. Technol. B **6**, 1678 (1988).

[23] Y. Shioya, T. Itoh, S. Inoue, and M. Maeda, J. Appl. Phys. **58**, 4194 (1985).

[24] E. J. McInerney, T. W. Mountsier, B. L. Chin, and E. K. Broadbent, J. Vac. Sci. Technol. B **11**, 734 (1993).